



ORIGINAL ARTICLE

p53 mutation regulates PKD genes and results in co-occurrence of PKD and tumorigenesis

Haili Li^{1,2*}, Yongjin Zhang^{2*}, Juhua Dan², Ruoyu Zhou², Cui Li², Rong Li³, Xiaoming Wu², Sanjay Kumar Singh⁴, Jeffrey T. Chang⁵, Julun Yang⁶, Ying Luo^{1,2}

¹Faculty of Environmental Science and Engineering, Kunming University of Science and Technology, Kunming 650500, China; ²Laboratory of Molecular Genetics of Aging & Tumor, Kunming University of Science and Technology, Kunming 650500, China; ³Division of Nephrology, The First People's Hospital of Yunnan Province, Kunming 650032, China; ⁴Department of Cancer Systems Imaging, The University of Texas MD Anderson Cancer Center, Houston 77030, TX, USA; ⁵Department of Integrative Biology and Pharmacology, University of Texas Health Science Center at Houston, Houston 77030, TX, USA; ⁶Department of Pathology, Kunming General Hospital, Kunming 650032, China

ABSTRACT

Objective: Polycystic kidney disease (PKD) is the major cause of kidney failure and mortality in humans. It has always been suspected that the development of cystic kidney disease shares features with tumorigenesis, although the evidence is unclear.

Methods: We crossed p53 mutant mice (p53N236S, p53S) with Werner syndrome mice and analyzed the pathological phenotypes. The RNA-seq, ssGSEA analysis, and real-time PCR were performed to dissect the gene signatures involved in the development of disease phenotypes.

Results: We found enlarged kidneys with fluid-filled cysts in offspring mice with a genotype of *G3mTerc^{-/-}WRN^{-/-}p53^{S/S}* (G3TM). Pathology analysis confirmed the occurrence of PKD, and it was highly correlated with the incidence of tumorigenesis. RNA-seq data revealed the gene signatures involved in PKD development, and demonstrated that PKD and tumorigenesis shared common pathways, including complement pathways, lipid metabolism, mitochondria energy homeostasis and others. Interestingly, this G3TM PKD and the classical PKD1/2 deficient PKD shared common pathways, possibly because the mutant p53S could regulate the expression levels of PKD1/2, *Pkhd1*, and *Hnf1b*.

Conclusions: We established a dual mouse model for PKD and tumorigenesis derived from abnormal cellular proliferation and telomere dysfunction. The innovative point of our study is to report PKD occurring in conjunction with tumorigenesis. The gene signatures revealed might shed new light on the pathogenesis of PKD, and provide new molecular biomarkers for clinical diagnosis and prognosis.

KEYWORDS

p53 mutation; telomere dysfunction; polycystic kidney disease; tumorigenesis

Introduction

Polycystic kidney disease (PKD) is a disease where enlarged kidneys develop characteristic fluid-filled cysts. Cysts in the liver or pancreas, cerebral aneurysms, abnormal cardiac development, and hypertension are also frequently found in PKD patients. Genetic studies have shown that

approximately 80% of autosomal dominant PKD (ADPKD) is caused by mutations in the PKD1 gene (encoding polycystin-1, PC1), and about 20% of ADPKD was due to mutations in PKD2 gene (encoding polycystin-2, PC2). It has been extensively shown that PC1/2 act as the key regulators for calcium homeostasis, and the dysfunction of PC1/2 might play an essential role in calcium imbalance and cAMP signaling, resulting in the development of PKD phenotypes^{1,2}. Increasing evidence suggests that PC1/2 proteins might interact with key regulators in cell cycle regulation, especially in cell proliferation and secretion-related signaling pathways¹. PKD1 has been found to play a role in preventing immortalized proliferation of renal cells through p53 and JNK, suggesting a novel link between PKD1

*These authors contributed equally to this work.

Correspondence to: Julun Yang and Ying Luo

E-mail: yingluo@kmust.edu.cn and yangjulun@sina.com

Received July 6, 2018; accepted November 8, 2018.

Available at www.cancerbiomed.org

Copyright © 2019 by Cancer Biology & Medicine

and p53³. It has also been found that the tumor suppressor protein p53 participates in a negative feedback loop to regulate PKD1 gene expression, thus preventing renal cysts formation⁴. Interestingly, another study has shown that Mekk1 acts as a co-repressor with p53 to downregulate PKD1 transcription. This PKD1 repression could be promoted by stress stimuli, suggesting that abnormally elevated stress responses might directly downregulate the PKD1 gene, possibly causing haploinsufficiency and cyst formation⁵. In an endothelial cell-culture system, elevated expression of mechanosensory polycystins in human carotid atherosclerotic plaques is associated with p53 activation and disease severity⁶. At the animal level, Bcl2 knockout mice manifested PKD and PKD phenotypes that could not have been rescued by p53 deficiency^{7,8}. The mutant p53 protein, especially the missense point mutation, is the major form of p53 deficiency in human disease. It promotes the progress of disease by both loss and gain of function⁹. However, no evidence has been found to connect mutant p53 with the progress of PKD.

Werner syndrome (WS) protein is a member of the RecQ helicase family implicated in the maintenance of genome stability. WRN plays an essential role in telomere DNA replication, and WRN defects cause human pathologies linked to cancer predisposition and premature aging, such as WS¹⁰⁻¹². By masking the chromosome ends from the DNA repair machinery through repression of the ATM/ATR signaling pathways, telomere DNA has a crucial function in DNA damage response (DDR). Telomere DNA is elongated by telomerase and protected by the protein complex shelterin, which regulates telomere length and protects telomeres from activating DDR¹³.

The mouse model of WS is established by double knockout of WRN and the RNA component of telomerase. The late generation (G4-6) of WS mice with both telomerase and WRN deficiency (*mTR*^{-/-}*WRN*^{-/-}) exhibited the clinical features observed in WS patients¹⁴⁻¹⁶. Our previous study has shown that ALT tumorigenic cell lines derived from senescent WS MEFs gained the same point mutation in tumor suppressor gene *Trp53*, encoding a mutant p53 protein known as p53N236S (p53S hereafter). The p53^{S/S} mice manifested highly invasive lymphomas and metastatic sarcomas with dramatically increased double minute chromosomes¹⁷.

We introduced this p53S mutation back into WS mice to study the intrinsic role of p53S in modulating WS symptoms, by crossing mice carrying p53S mutation with WS mice. Surprisingly, we found that the offspring of p53S and WS mice (*mTR*^{-/-}*WRN*^{-/-}*p53*^{S/S}) manifested both PKD and tumor phenotypes. Here we report the phenotypes of this novel

mouse model. By RNA-seq and ssGSEA analysis, we have identified the gene signatures and pathways that connect mutant p53 and telomere dysfunction with the development of PKD.

Materials and methods

Mice

Transgenic p53S mice and WS (*mTR*^{-/-}*WRN*^{-/-}) mice were bred to generate *mTR*^{-/-}*WRN*^{-/-}*p53*^{S/S} mice. We crossed mice carrying p53S mutation (*p53*^{S/S}) with WS mice (*mTR*^{-/-}*WRN*^{-/-}) and obtained the first generation of mice with telomerase knockout, WRN knockout, and p53S mutation (G1 *mTR*^{-/-}*WRN*^{-/-}*p53*^{S/S}), referred to as G1 triple mutation (G1TM). The mice were then bred generation-by-generation to obtain G2 and G3 TM mice. The telomerase knockout and WRN knockout mice (double mutation, DM) and wild type (WT) mice were used as control. All experiments were carried out with the approval of the Kunming University of Science and Technology and Use Committee (Approval ID: M2015-011) in accordance with the guidelines of the Association for Assessment and Accreditation of Laboratory Animal Care.

MEF cells

The MEF cells with different genotypes were harvested in 13.5 days and cultured in Dulbecco's modified Eagle's medium (DMEM) with 10% fetal bovine serum (FBS) at 37 °C with 5% CO₂ and 3% O₂. To maintain their original characteristics, only the early passages (≤ passage 5) of MEF cells were used for experiments.

Pathology analysis

Mouse kidney samples were fixed in 4% neutral buffered formalin for 6 hours, then alcohol-dehydrated and paraffin-embedded. The paraffin-embedded tissue blocks were sectioned into 4 μm slices for later experiments. For hematoxylin-eosin (HE) staining, the tissue sections were deparaffinized and rehydrated, and H&E staining was applied. The H&E stained slides were observed via microscopy and the histological changes and kidney lesions were evaluated by pathologists.

RNA-seq and gene expression signature analysis

Cell or tissue (sarcoma and cystic kidney) samples were collected and sent for commercial RNA-seq service

(Novogene, China). Briefly, the total RNA was extracted and enriched by oligo-dT labeled magnetic beads, and used to construct a library for RNA-seq. The sequenced reads (raw reads) were evaluated for quality control. The adapters and low quality reads were filtered to obtain clean reads. The clean data were then aligned with the reference mouse genome by TopHat2. The RNA-seq counts were annotated and the FPKM file was generated for bioinformatic analysis.

The Bioinformatics ExperT SYstem (BETSY) was applied to automate the development of workflows¹⁸. The single sample gene set enrichment analysis (ssGSEA)¹⁹ was applied to analyze the RNA-seq data. Hallmark (designed for well-defined biological states and processes), C2 (BIOCARTA, KEGG, REACTOME, etc.), and C5 (GO) gene sets from the Molecular Signatures Database²⁰ were used for ssGSEA analysis. The heat maps were plotted with BETSY by centering with mean but without hierarchical clustering. The common pathways between cystic kidneys and tumors were ranked and plotted based on their ssGSEA scores.

Ingenuity pathway analysis

The essential genes involved in PKD development were selected according to the literature^{1,21}. The fold change in their expression between G3TM and G3DM was calculated from RNA-seq data. After applying the cutoff (2 ×) for gene expression fold change, the remaining genes and their fold changes, and *P* values were imported to Ingenuity Pathway Analysis (IPA) software. The knowledge base of IPA were used to draw their expression regulation and interaction network. The network with largest numbers of genes is included, such as developmental disorders, immunological diseases, inflammatory diseases, inflammatory response, and renal and urological disease.

Quantitative real-time PCR analysis

RNA was isolated from cell or tissue samples, and cDNA was synthesized by reverse transcription. Real-time PCR was performed on an ABI Prism 7300 sequence detection system with SYBR-Green PCR master mix according to the manufacturer's instructions (Applied Biosystems, CA). The primers used are as follows:

PKD1, forward primer: 5'-CCCTCTCGGAGCAGAA TCAAT-3', reverse primer: 5'-GTGTTGAGCTAATGGGC AGG-3';

PKD2, forward primer: 5'-GGGGAACAAGACTCATG GAAG-3', reverse primer: 5'-GCCGTAGGTCAAGATGC ACAA-3';

Pkhd1, forward primer: 5'-GGGAGGTTCGATGGTGCA

TAAG-3', reverse primer: 5'-GATGTCCGTTCTTCCCCC AAG-3';

Hnf1b, forward primer: 5'-AGGGAGGTGGTCGATG TCA-3', reverse primer: 5'-TCTGGACTGTCTGGTTGA ACT-3';

C2, forward primer: 5'-CGGTGGTAATTTACCCCTCAG-3', reverse primer: 5'-GGTGTGATGTGAGCTAGACCT-3';

C5, forward primer: 5'-GAACAAACCTACGTCATTTCA GC-3', reverse primer: 5'-GTCAACAGTGCCGCGTTTT-3';

Pgc1a, forward primer: 5'-TATGGAGTGACATAGAGTGT GCT-3', reverse primer: 5'-CCACTTCAATCCACCCAGAAA G-3';

Tfam, forward primer: 5'-ATTCCGAAGTGTTTTTC CAGCA-3', reverse primer: 5'-TCTGAAAGTTTTGCATCTG GGT-3';

Wnt1, forward primer: 5'-GGTTTCTACTACGTTGCTA CTGG-3', reverse primer: 5'-GGAATCCGTCAACAGGTT CGT-3';

Ctnnb1, forward primer: 5'-ATGGAGCCGGACAGAAA AGC-3', reverse primer: 5'-CTTGCCACTCAGGGAAG GA-3';

Srebf1, forward primer: 5'-GATGTGCGAACTGGACA CAG-3', reverse primer: 5'-CATAGGGGGCGTCAAAC AG-3';

Srebf2, forward primer: 5'-GCAGCAACGGGACCAT TCT-3', reverse primer: 5'-CCCCATGACTAAGTCCCTCAA CT-3';

β-actin, forward primer: 5'-AGAGGGAAATCGTGCG TGAC-3', reverse primer: 5'-CAATAGTGATGACCTGGCC GT-3'.

Results

Generation of a mouse model manifesting PKD phenotypes

We crossed mice carrying p53S mutation with WS mice and obtained the first generation of mice with telomerase, *WRN* knockout, and p53S mutations (*G1mTR^{-/-}WRN^{-/-}p53^{S/S}*), referred to as G1 triple mutation (G1TM). The mice were then bred generation-by-generation to obtain G2 and G3 TM mice (**Figure 1A** and **1B**).

As expected, we observed the incidence of sarcomas when telomere length was shortened to a certain level, which occurred in G3TM (*G3mTR^{-/-}WRN^{-/-}p53^{S/S}*) mice (**Figure 1C**). The affected mice were sacrificed and anatomical analysis showed that the mice also manifested unilateral or bilateral enlarged kidneys with multiple fluid-filled cysts (**Figure 1D**). Thus, surprisingly, PKD phenotypes were found in G3TM mice at around 4 months old.

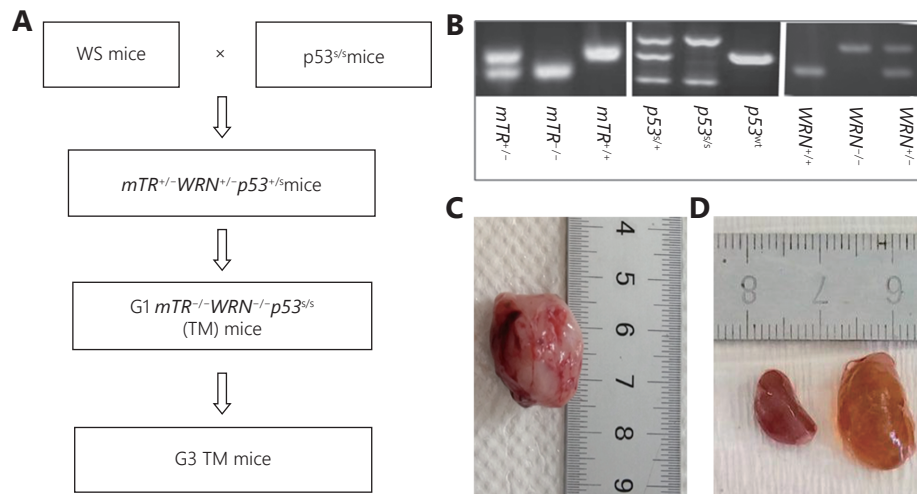


Figure 1 Generation of a mouse model manifesting PKD. (A) The breeding strategy for generating G3TM ($G3mTR^{-/-}WRN^{-/-}p53^{S/S}$). Mice carrying the p53S mutation were crossed with WS mice and G1TM were obtained ($G1mTR^{-/-}WRN^{-/-}p53^{S/S}$). The mice were then bred generation-by-generation to obtain G2 and G3 TM mice. (B) Genotyping of mice carrying mTR, WRN and p53S mutations. (C) Incidence of sarcoma in a G3TM mouse. (D) Bilateral enlarged kidneys with multiple fluid-filled cysts in a G3TM mouse.

The H&E of the kidney sections showed that the kidneys from wild type mice developed normal renal tubules and glomeruli (**Figure 2A**), while the kidneys from G3TM mice displayed a range of phenotypes associated with renal dysplasia and renal cyst formation. In the G3TM mouse EH85, the normal histological structure of the right kidney

was completely replaced by fluid-filled cysts of various sizes (**Figure 2B**). At higher magnification, we could observe that the renal tubules and glomeruli were compressed and atrophied, and the glomerulus lost its capillary loop structure completely (**Figure 2C**). These data show the severe fluid-filled cyst formation and total loss of renal function in this

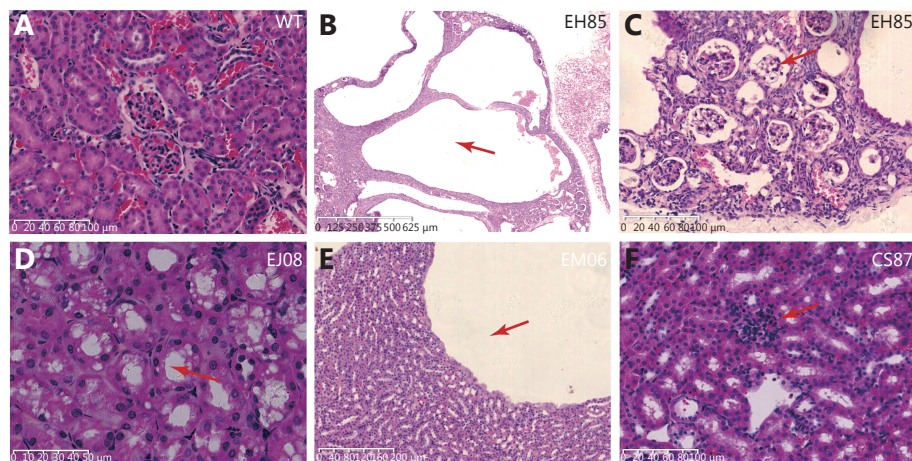


Figure 2 Hematoxylin and eosin staining of kidney sections from mice with PKD phenotype. (A) The normal morphology of a kidney from a wild type mouse. (B) An end stage cystic kidney from a G3TM ($G3mTR^{-/-}WRN^{-/-}p53^{S/S}$) mouse (ID number: EH85). The normal structure was completely replaced by various sizes of fluid-filled cysts (arrow pointed). (C) Higher magnification power view of the cystic kidney from mouse EH85 showing that the renal tubules and glomeruli were compressed and atrophied. The glomerulus was enclosed and lost its capillary loop structure (arrow pointed). (D) Swelling renal tubule epithelial cells, hydropic degeneration, and vacuolation in the cells were observed (arrow pointed) in the kidney from G3TM mouse EJ08. (E) A kidney from the G3TM mouse EM06, showing the cyst surrounding flat epithelial cells (arrow pointed) that might be caused by fluid pressure changes resulting from cyst formation. (F) An abnormal glomerulus with poorly defined capillary loop (arrow pointed) in the kidney from G3TM mouse CS87.

kidney. In the kidney from G3TM mouse EJ08, cellular swelling or hydropic degeneration and vacuolation were observed (**Figure 2D**), suggesting the dysfunction of ion and water regulation in these renal cells. In the kidneys from G3TM mouse EM06, the cyst is surrounded by flat epithelial cells, which suggests that cellular morphological changes are caused by fluid pressure from the cyst (**Figure 2E**). In the kidney from G3TM mouse CS87, we found the abnormal glomerulus with poorly defined capillary loop (**Figure 2F**). The abnormal glomerulus with semi-enclosed capillary loop was also frequently observed, indicating the loss of glomerulus function and downregulation of blood filtering function.

Together these data suggest that kidneys from *G3mTR^{-/-}WRN^{-/-}p53^{S/S}* mice were hypoplastic and developed PKD phenotypes.

The correlation of tumorigenesis and PKD phenotypes

As described earlier, the G3TM mice should manifest phenotypes that correlate with abnormal DNA damage response and abnormal proliferation. In our case, it manifested as increased tumorigenesis and PKD formation. To further understand the relationship between abnormal DNA damage response, tumorigenesis, and PKD phenotypes, we analyzed the frequencies and co-occurrence of cystic kidney and tumorigenesis in mice groups with different genotypes.

We did not find any tumorigenesis or PKD in those mice with WRN and telomerase double knockout, including G1DM mice ($n=41$), G2DM mice ($n=52$), and G3DM ($n=63$). However, we observed a few PKD or tumor incidences in G1TM and G2TM mice; this number increased dramatically in G3TM mice (**Table 1, Figure 3A**). The incidence increased along with telomere shortening (G1-G2-G3) and the introduction of p53S (TM vs. DM). These data strongly suggest that interplay of telomere DNA damage and p53S mutation contributed to the development of PKD. Furthermore, most PKD co-occurred with tumor phenotypes (**Table 1, Figure 3A**), showing that the occurrence of PKD

phenotype was highly correlated with increased tumorigenesis.

Gene signatures of PKD caused by telomere dysfunction and p53S mutation

Since the genetic defect in this PKD model is very different from classical PKD models with polycystins defects, we were interested in investigating the gene signatures in MEFs (G3TM), cystic kidneys, and tumors from G3TM. We compared the gene expression profiles in MEFs from G1DM to G3TM mice using RNA-seq and ssGSEA analysis, as well as the tumors and cystic kidneys from G3TM mice.

First, we analyzed the gene signatures that were upregulated or downregulated in cystic kidneys using the Hallmark dataset. We found that the metabolism-related pathways, particularly lipid metabolism, were strikingly upregulated in cystic kidneys. These included bile acid metabolism, fatty acid metabolism and others (**Figure 3B**). Cell cycle-related pathways were clearly downregulated, such as mitotic spindle, G2M checkpoint, and E2F targets. (**Figure 3B**). These data suggest that abnormal metabolic regulation contributed greatly to PKD progress in G3TM mice.

Interestingly, the pathways such as oxidative phosphorylation, complement, and interferon alpha gamma were upregulated in both cystic kidneys and tumors (**Figure 3B**). These common regulated pathways suggest that the development of cystic kidney shares common mechanisms with tumorigenesis.

We then expanded the ssGSEA analysis by combining the Hallmark, C2, and C5 datasets²⁰, and mapping the gene signatures that were gradually upregulated or downregulated in G3TM cells, tumors, and cystic kidneys (**Supplementary Figure S1 and S2**). The data revealed that most strikingly upregulated pathways shared by tumors and cystic kidneys included complement pathways, the immune response, lipid metabolism, and mitochondrial energy homeostasis. Interestingly, we observed that kidney function-related pathways, such as microvillus organization and water homeostasis, were upregulated in both tumors and kidneys. The data also show that organic cation transport and

Table 1 The occurrence of cystic kidney and/or tumor in mice with different genotypes

Number of mice	G1DM	G1 TM	G2 DM	G2 TM	G3 DM	G3 TM
Cystic kidney	0	1	0	2	0	4
Tumor	0	5	0	9	0	23
Cystic kidney+ tumor	0	5	0	9	0	23
Total	41	21	52	39	63	43

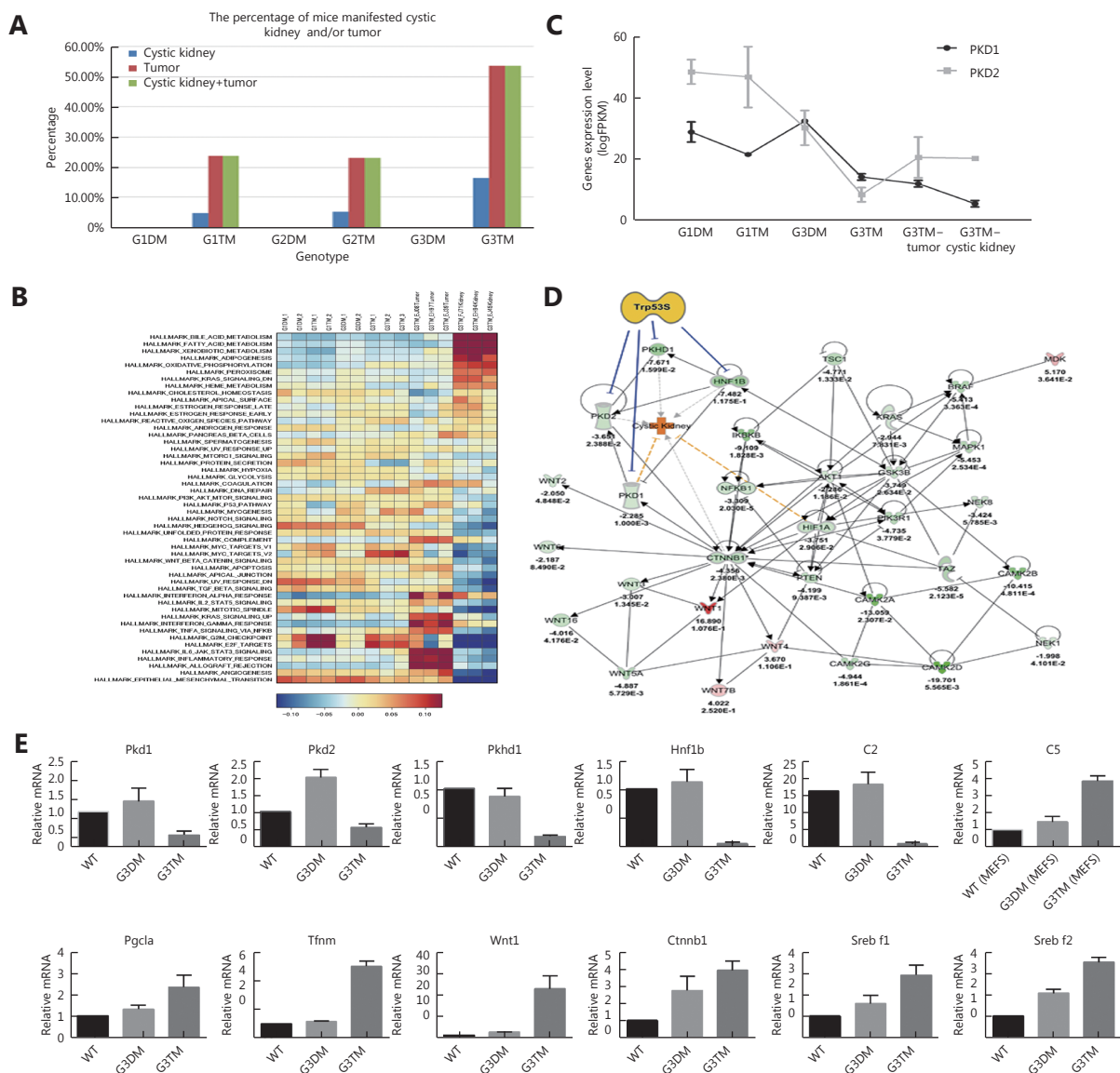


Figure 3 Co-occurrence of tumorigenesis with PKD and gene signature analysis. (A) The percentage of tumor/cystic kidney incidence in mice with genotypes from G1DM ($G1mTR^{-/-}WRN^{-/-}$) to G3TM ($G3mTR^{-/-}WRN^{-/-}p53^{S/S}$) indicated the co-occurrence of tumorigenesis with PKD, and the incidence increased with telomere shortening (G1-G2-G3), and the introduction of p53S (TM vs. DM). (B) The heatmap of gene expression profiles (ssGSEA analysis results of the RNA-seq data using Hallmark dataset) in MEFs from G1DM, G2DM, G3DM, G1TM, G2TM, and G3TM mice, as well as the tumors and cystic kidneys from G3TM mice. The pathways were ranked by scores showing up- (red) or downregulation (blue) in cystic kidney, as well as in tumor and in G3TM MEFs. (C) The expression levels of PKD1 and PKD2 decreased significantly from G1DM to G3TM, along with the introduction of p53S mutation and telomere shortening. (D) The interaction network of genes essential for classical PKD development generated by Ingenuity Pathway Analysis (IPA). The expression fold change and P -values are shown under the gene name. Genes downregulated by Trp53S are connected by blue inhibition lines. As per IPA knowledge base, orange lines indicate gene expression level is consistent with activation of cystic kidney, whereas grey lines are inconsistent with activation of cystic kidney. (E) The validation of key gene expression levels by quantitative real-time PCR. The expression levels of genes involved in PKD pathway (PKD1, PKD2, Pkd1, Hnf1b), complement pathway (C2 and C5), mitochondria pathway (Pgc1a and Tfam), Wnt signaling pathway (Wnt1 and Ctnnb1), and lipid metabolism pathway (Sreb1 and Sreb2) were evaluated by real-time PCR in G3TM MEFs. WT MEFs and G3DM MEFs were used as controls.

glucuronidation pathways were highly upregulated in cystic kidneys (**Supplementary Figure S1**).

On the other hand, the pathways obviously downregulated in tumor and kidneys included cytoskeleton regulation, extracellular signal transduction and others (**Supplementary Figure S2**). Together, regulation of these pathways revealed that G3TM PKD shares common mechanisms with tumorigenesis. These dysfunctions of gene regulation composed the gene signatures of G3TM PKD.

Comparison of gene signatures in PKD caused by telomere dysfunction and p53S mutation with classical PKD caused by PKD1 or PKD2 deficiency

After analyzing the gene signatures in the G3TM PKD model (*G3mTR^{-/-}WRN^{-/-}p53^{S/S}*), we compared the gene signatures in this model with classic PKD models with PKD1 or PKD2 deficiency. We analyzed RNA-seq data of the classic PKD models with PKD1 or PKD2 deficiency²² by the same ssGSEA analysis, and compared gene signatures between the three mouse models. The data, analyzed by the Hallmark dataset, showed that the common upregulated pathways among these three PKD models included complement, coagulation, and apical surface, whereas the common downregulated pathways included angiogenesis (**Supplementary Table S1**).

The expanded analysis with Hallmark, C2, and C5 datasets revealed that common upregulated pathways included complement activation, bile acid metabolism, and ion homeostasis. The common downregulated pathways included cell-to-cell adhesion signaling and epithelial structural maintenance (**Supplementary Table S2**).

Together these data reveal that although the G3TM PKD model was derived from different genetic aberrations to classical PKD models, they share common pathways in regulating complement activation, lipid metabolism, cell-to-cell adhesion signaling etc. These pathways might play an essential role in PKD development.

Furthermore, we found that from G1DM to G3TM, along with the introduction of p53S mutation and telomere shortening, the expression levels of PKD1 and PKD2 decreased significantly (**Figure 3C**), suggesting that p53S mutation could downregulate PKD1 and PKD2 expression. In the end-stage tumor and cystic kidney tissues, the PKD2 level was slightly upregulated, but was still lower than the level in G3DM (**Figure 3C**).

Since G3TM is the genotype with most incidences of tumor and cystic kidney disease, but not G3DM, comparison of gene regulation in G3TM with G3DM might provide the

mechanisms for PKD attributed to p53S. We evaluated the genes essential for classical PKD development^{1,21}, and mapped their interaction networks with IPA (**Figure 3D**). Based on expression fold-changes of genes in this interaction network, the molecule activity predictor showed that cystic kidney module was significantly activated (*P*-value: 3.31E-11). Other than PKD1 and PKD2, the ARPKD protein Pkhd1 (polyductin) and its transcriptional factor Hnf1b (hepatocyte nuclear factor 1 homeobox B)²³ were also downregulated. These data suggest that p53S plays a role in transcriptional regulation of PKD-related genes.

To validate the key genes in altered pathways as revealed by RNA-seq data, we further analyzed the regulation of genes involved in the PKD pathway, complement pathway, mitochondria pathway, Wnt signaling pathway, and lipid metabolism pathway by quantitative real-time PCR. Compared with WT and G3DM MEFs, the expression of PKD genes PKD1, PKD2, Pkhd1, and Hnf1b was suppressed in G3TM MEFs. However, complement pathway genes C2 and C5; mitochondria pathway genes Pgc1a and Tfam; Wnt signaling pathway genes Wnt1 and Ctnnb1; and lipid metabolism pathway genes Srebf1 and Srebf2 were upregulated in G3TM MEFs (**Figure 3E**). These data further confirmed the RNA-seq data, and suggest that p53S regulates genes involved in the aforementioned pathways attributed to the development of cystic kidney.

Discussion

It has always been suspected that the development of cystic kidney disease shares features with tumorigenesis, although the evidence is unclear^{24,25}. Recent understanding of aberrant downstream pathways in ADPKD demonstrates that transcriptional functions that regulate cell cycle progression, energy metabolism, and secretion-related signaling are abnormal in PKD¹, and p53 is the essential node in all these transcriptional regulations²⁶.

It has always been documented that wild type p53 could bind to the PKD1 promoter, and the kidneys of p53 null mice expressed higher PKD1 mRNA levels than wild-type littermates, suggesting that wild type p53 suppressed the expression of PKD1⁴. It has also been shown that depletion of PKD1 led to increased cell proliferation and caused a premature G1/S transition, and the elevated expression of mechanosensory polycystins in human carotid atherosclerotic plaques was associated with p53 activation^{6,27}. Thus, it is conceivable that mutant p53, which loses the wild type function of p53 and gains oncogenic function, plays an important role in the development of PKD.

Here we revealed a novel PKD and tumor combined mouse model (PKD derived from $G3mTR^{-/-}WRN^{-/-}p53^{S1/S}$ mice) (Figure 1 and 2). The co-occurrence of cystic kidneys and tumors suggests common genetic mechanisms, which in this case could be DNA damage caused by telomere dysfunction and the abnormal DNA damage response, cellular proliferation, or metabolic dysregulation caused by p53N236S mutation. This model provides direct evidence to connect mutant p53 DNA damage response with PKD development. The fact that the incidences of cystic kidneys increased along with telomere shortening suggests that DNA damage triggered the development of PKD.

To dissect the common genetic causes of PKD and tumorigenesis, we identified the upregulated pathways in tumors and cystic kidneys. Among the common pathways in cystic kidneys and tumors, the pathways of activation of complement, inflammatory response, and mitochondrial function were most significantly upregulated (Figure 3B and 3E, Supplementary Figure S1). It has been documented that activation of the alternative complement pathway and the consequent inflammatory response plays an essential role in the progress of kidney diseases, such as atypical hemolytic uremic syndrome, C3 glomerulopathies, and atypical post

infectious GN, as well as ADPKD^{28,29}. These data suggest the importance of complement cascade in the regulation of inflammatory response of both cystic kidney disease and tumors.

Mitochondrial function is essential in energy metabolism, oxygen consumption, ROS regulation, and ATP synthesis. Aside from kidney disease, mitochondrial dysfunction is also related to the processes of aging and tumor development^{30,31}. By ssGSEA analysis, we found that the pathways involved in mitochondrial function and related fatty acid metabolisms are highly activated in tumors and cystic kidneys from G3TM mice; however, they are not significantly up-regulated in PKD1- or PKD2-deficient PKD²²(Supplementary Table S1, S2).

It is very promising that we found that PKD1, PKD2, Pkhd1, and Hnf1b were all downregulated by the introduction of p53S (Figure 3D). It has been documented that Hnf1b is the transcription factor for both Pkhd1 and PKD2. Mutation of Hnf1b results in kidney phenotypes that include renal agenesis, dysplasia, and cysts³². These phenotypes are consistent with our pathological analysis (Figure 2).

Putting these data together, we report a novel PKD and

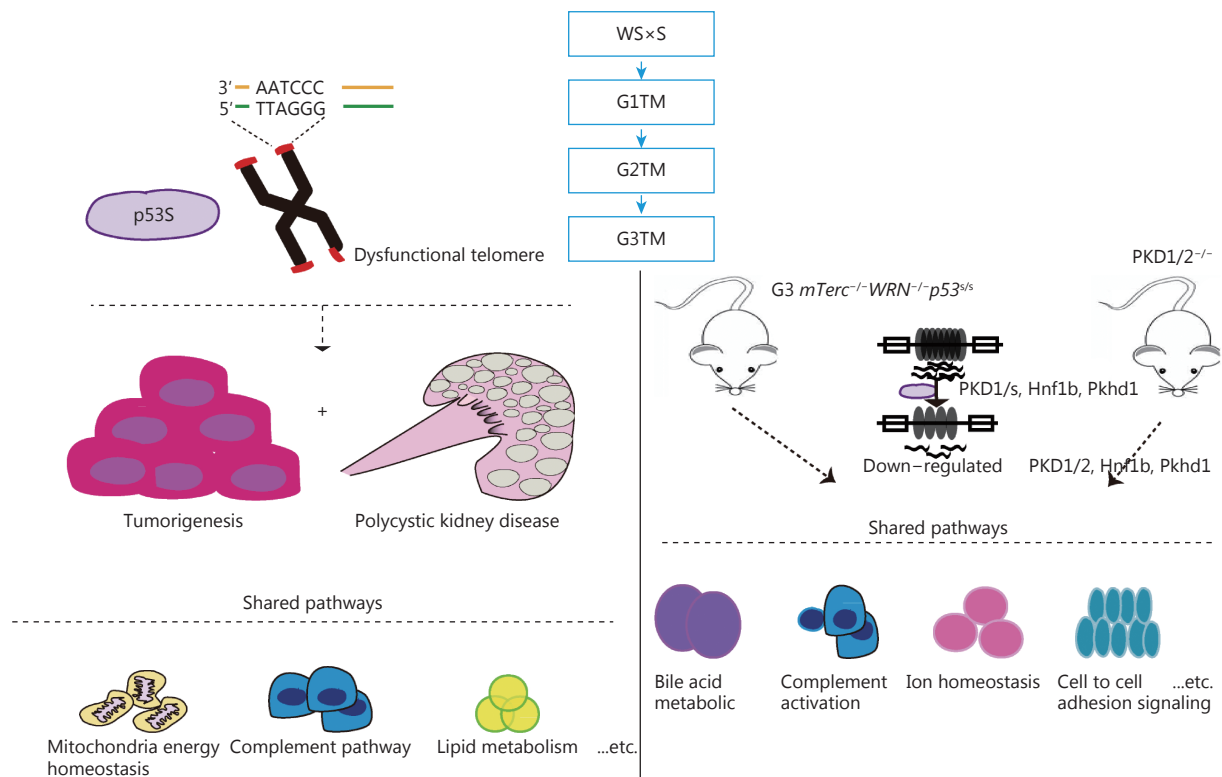


Figure 4 A schematic of the establishment of G3TM PKD model, and the gene signatures shared between development of PKD and tumorigenesis, and with PKD1/2 PKD model.

tumor combined mouse model, and reveal the gene signatures involved in the development of PKD. The G3TM PKD model shared common pathways with classical PKD. These common pathways might be essential in PKD progress, and thus could be common targets for PKD prevention, drug screening, and patient care strategies. In depth analyses of these pathways could provide new biomarkers for the clinical diagnosis and prognosis of PKD (**Figure 4**).

Acknowledgements

This work was supported by National Natural Science Foundation of China (NSFC) (Grant No. 30771194 and 31170735). We thank Dr. Sandy Chang from Yale University and Dr. Ronald A Depinho from The University of Texas MD Anderson Cancer Center for kindly providing WS mice.

Conflict of interest statement

No potential conflicts of interest are disclosed.

References

- Harris PC, Torres VE. Genetic mechanisms and signaling pathways in autosomal dominant polycystic kidney disease. *J Clin Invest*. 2014; 124: 2315-24.
- Mangolini A, de Stephanis L, Aguiari G. Role of calcium in polycystic kidney disease: From signaling to pathology. *World J Nephrol*. 2016; 5: 76-83.
- Nishio S, Hatano M, Nagata M, Horie S, Koike T, Tokuhisa T, et al. Pkd1 regulates immortalized proliferation of renal tubular epithelial cells through p53 induction and JNK activation. *J Clin Invest*. 2005; 115: 910-8.
- Van Bodegom D, Saifudeen Z, Dipp S, Magenheimer BS, Calvet JP, et al. The polycystic kidney disease-1 gene is a target for p53-mediated transcriptional repression. *J Biol Chem*. 2006; 281: 31234-44.
- Islam MR, Jimenez T, Pelham C, Rodova M, Puri S, Magenheimer BS, et al. MAP/ERK kinase kinase 1 (MEKK1) mediates transcriptional repression by interacting with polycystic kidney disease-1 (PKD1) promoter-bound p53 tumor suppressor protein. *J Biol Chem*. 2010; 285: 38818-31.
- Varela A, Piperi C, Sigala F, Agrogiannis G, Davos CH, Andri MA, et al. Elevated expression of mechanosensory polycystins in human carotid atherosclerotic plaques: Association with p53 activation and disease severity. *Sci Rep*. 2015; 5: 13461.
- Li X, Miao X, Wang HS, Xu ZX, Li B. The tissue dependent interactions between p53 and Bcl-2 in vivo. *Oncotarget*. 2015; 6: 35699-709.
- Weis DJ, Sorenson CM, Shutter JR, Korsmeyer SJ. Bcl-2-deficient mice demonstrate fulminant lymphoid apoptosis, polycystic kidneys, and hypopigmented hair. *Cell*. 1993; 75: 229-40.
- Kim MP, Lozano G. Mutant p53 partners in crime. *Cell Death Differ*. 2018; 25: 161-8.
- Chu WK, Hickson ID. Recq helicases: Multifunctional genome caretakers. *Nat Rev Cancer*. 2009; 9: 644-54.
- Ozgenç A, Loeb LA. Werner syndrome, aging and cancer. *Genome Dyn*. 2006; 1: 206-17.
- Crabbe L, Verdun RE, Haggblom CI, Karlseder J. Defective telomere lagging strand synthesis in cells lacking wrn helicase activity. *Science*. 2004; 306: 1951-3.
- Palm W, de Lange T. How shelterin protects mammalian telomeres. *Annu Rev Genet*. 2008; 42: 301-34.
- Lebel M, Leder P. A deletion within the murine werner syndrome helicase induces sensitivity to inhibitors of topoisomerase and loss of cellular proliferative capacity. *Proc Natl Acad Sci USA*. 1998; 95: 13097-102.
- Chang S, Multani AS, Cabrera NG, Naylor ML, Laud P, Lombard D, et al. Essential role of limiting telomeres in the pathogenesis of werner syndrome. *Nat Genet*. 2004; 36: 877-82.
- Du XB, Shen J, Kugan N, Furth EE, Lombard DB, Cheung C, et al. Telomere shortening exposes functions for the mouse werner and bloom syndrome genes. *Mol Cell Biol*. 2004; 24: 8437-46.
- Zhao LJ, Wang BY, Zhao XL, Wu XM, Zhang QS, Wei CY, et al. Gain of function in the mouse model of a recurrent mutation p53N236S promotes the formation of double minute chromosomes and the oncogenic potential of p19ARF. *Mol Carcinog*. 2018; 57: 147-58.
- Chen X, Chang JT. Planning bioinformatics workflows using an expert system. *Bioinformatics*. 2017; 33: 1210-5.
- Subramanian A, Tamayo P, Mootha VK, Mukherjee S, Ebert BL, Gillette MA, et al. Gene set enrichment analysis: A knowledge-based approach for interpreting genome-wide expression profiles. *Proc Natl Acad Sci USA*. 2005; 102: 15545-50.
- Liberzon A, Subramanian A, Pinchback R, Thorvaldsdottir H, Tamayo P, Mesirov JP. Molecular signatures database (MSigDB) 3.0. *Bioinformatics*. 2011; 27: 1739-40.
- Ong ACM, Harris PC. A polycystin-centric view of cyst formation and disease: The polycystins revisited. *Kidney Int*. 2015; 88: 699-710.
- Woo YM, Kim DY, Koo NJ, Kim YM, Lee S, Ko JY, et al. Profiling of miRNAs and target genes related to cystogenesis in ADPKD mouse models. *Sci Rep*. 2017; 7: 14151.
- Gresh L, Fischer E, Reimann A, Tanguy M, Garbay S, Shao XL, et al. A transcriptional network in polycystic kidney disease. *EMBO J*. 2004; 23: 1657-68.
- Kovács J, Gomba S, Zilahy M. Comparison of the morphology of renal cysts and cystic renal tumors. *Pathol Oncol Res*. 1997; 3: 272-7.

25. Lanoix J, D'Agati V, Szabolcs M, Trudel M. Dysregulation of cellular proliferation and apoptosis mediates human autosomal dominant polycystic kidney disease (ADPKD). *Oncogene*. 1996; 13: 1153-60.
 26. Kasthuber ER, Lowe SW. Putting p53 in context. *Cell*. 2017; 170: 1062-78.
 27. Kim H, Bae Y, Jeong W, Ahn C, Kang S. Depletion of PKD1 by an antisense oligodeoxynucleotide induces premature G1/S-phase transition. *Eur J Hum Genet*. 2004; 12: 433-40.
 28. De Vriese AS, Sethi S, Van Praet J, Nath KA, Fervenza FC. Kidney disease caused by dysregulation of the complement alternative pathway: An etiologic approach. *J Am Soc Nephrol*. 2015; 26: 2917-29.
 29. Su Z, Wang X, Gao X, Liu Y, Pan C, Hu H, et al. Excessive activation of the alternative complement pathway in autosomal dominant polycystic kidney disease. *J Intern Med*. 2014; 276: 470-85.
 30. Emma F, Montini G, Parikh SM, Salviati L. Mitochondrial dysfunction in inherited renal disease and acute kidney injury. *Nat Rev*. 2016; 12: 267-80.
 31. Bhargava P, Schnellmann RG. Mitochondrial energetics in the kidney. *Nat Rev*. 2017; 13: 629-46.
 32. Faguer S, Chassaing N, Bandin F, Prouheze C, Garnier A, Casemayou A, et al. The HNF1B score is a simple tool to select patients for HNF1B gene analysis. *Kidney Int*. 2014; 86: 1007-15.
- Cite this article as:** Li H, Zhang Y, Dan J, Zhou R, Li C, Li R, et al. p53 mutation regulates PKD genes and results in co-occurrence of PKD and tumorigenesis. *Cancer Biol Med*. 2019; 16: 79-88. doi: 10.20892/j.issn.2095-3941.2018.0170

Supplementary materials

Table S1 The common pathways shared by G3TM PKD and Pkd1/2-deficient PKD revealed by ssGSEA analysis results of the RNA-seq data using the Hallmark dataset

Up-regulated in G3TM PKD		Down-regulated in G3TM PKD	
Up-regulated in Pkd1 deficient PKD	Up-regulated in Pkd2 deficient PKD	Down-regulated in Pkd1 deficient PKD	Down-regulated in Pkd2 deficient PKD
HALLMARK_APICAL_SURFACE	HALLMARK_ANDROGEN_RESPONSE	HALLMARK_ANGIOGENESIS	HALLMARK_ANGIOGENESIS
HALLMARK_COAGULATION	HALLMARK_APICAL_SURFACE	HALLMARK_GLYCOLYSIS	HALLMARK_SPERMATOGENESIS
HALLMARK_COMPLEMENT	HALLMARK_CHOLESTEROL_HOMEOSTASIS	HALLMARK_MITOTIC_SPINDLE	
HALLMARK_ESTROGEN_RESPONSE_LATE	HALLMARK_COAGULATION	HALLMARK_MYOGENESIS	
HALLMARK_KRAS_SIGNALING_DN	HALLMARK_COMPLEMENT	HALLMARK_PI3K_AKT_MTOR_SIGNALING	
	HALLMARK_ESTROGEN_RESPONSE_EARLY	HALLMARK_UV_RESPONSE_DN	
	HALLMARK_ESTROGEN_RESPONSE_LATE		
	HALLMARK_INTERFERON_ALPHA_RESPONSE		
	HALLMARK_INTERFERON_GAMMA_RESPONSE		
	HALLMARK_PANCREAS_BETA_CELLS		
	HALLMARK_PROTEIN_SECRETION		

Table S2 The common pathways shared by G3TM PKD and Pkd1/2-deficient PKD revealed by ssGSEA analysis results of the RNA-seq data using Hallmark, C2, and C5 dataset

Up-regulated in G3TM PKD		Down-regulated in G3TM PKD	
Up-regulated in Pkd1 deficient PKD	Up-regulated in Pkd2 deficient PKD	Down-regulated in Pkd1 deficient PKD	Down-regulated in Pkd2 deficient PKD
AIGNER_ZEB1_TARGETS	AIGNER_ZEB1_TARGETS	AMIT_SERUM_RESPONSE_240_MCF10A	BECKER_TAMOXIFEN_RESISTANCE_UP
BANDRES_RESPONSE_TO_CARMUSTIN_WITHOUT_MGMT_24HR_UP	BIOCARTA_COMP_PATHWAY	BARIS_THYROID_CANCER_DN	BIOCARTA_CELL2CELL_PATHWAY
BIOCARTA_COMP_PATHWAY	BROWNE_HCMV_INFECTION_48HR_UP	BECKER_TAMOXIFEN_RESISTANCE_UP	BIOCARTA_GCR_PATHWAY
DACOSTA_UV_RESPONSE_VIA_ERCC3_COMMON_UP	DACOSTA_UV_RESPONSE_VIA_ERCC3_COMMON_UP	BIOCARTA_ELL2CELL_PATHWAY	BIOCARTA_NO2IL12_PATHWAY
DURCHDEWALD_SKIN_CARCINOGENESIS_UP	DURCHDEWALD_SKIN_CARCINOGENESIS_UP	BIOCARTA_IL2RB_PATHWAY	BIOCARTA_P53HYPOXIA_PATHWAY
FIGUEROA_AML_METHYLATION_CLUSTER_4_UP	ENGELMANN_CANCER_PROGENITORS_DN	BIOCARTA_SODD_PATHWAY	BIOCARTA_TALL1_PATHWAY
FURUKAWA_DUSP6_TARGETS_PCI35_UP	FIGUEROA_AML_METHYLATION_CLUSTER_4_UP	BOWIE_RESPONSE_TO_EXTRACELLULAR_MATRIX	BROWNE_INTERFERON_RESPONSIVE_GENES
GO_DE_NOVO_POSTTRANSLATIONAL_PROTEIN_FOLDING	FURUKAWA_DUSP6_TARGETS_PCI35_UP	BROWNE_INTERFERON_RESPONSIVE_GENES	CHAN_INTERFERON_PRODUCING_DENDRITIC_CELL
GO_DE_NOVO_PROTEIN_FOLDING	GO_DE_NOVO_POSTTRANSLATIONAL_PROTEIN_FOLDING	BURTON_ADIPOGENESIS_12	CHEMELLO_SOLEUS_VS_EDL_MYOFIBERS_DN
GO_2_IRON_2_SULFUR_CLUSTER_BINDING	GO_DE_NOVO_PROTEIN_FOLDING	CHAN_INTERFERON_PRODUCING_DENDRITIC_CELL	CHIANG_LIVER_CANCER_SUBCLASS_INTERFERON_UP
GO_AMMONIUM_ION_BINDING	GO_ACTIN_NUCLEATION	CHEMELLO_SOLEUS_VS_EDL_MYOFIBERS_DN	CLIMENT_BREAST_CANCER_COPY_NUMBER_UP
GO_APOPTOTIC_MITOCHONDRIAL_CHANGES	GO_APOPTOTIC_MITOCHONDRIAL_CHANGES	CLIMENT_BREAST_CANCER_COPY_NUMBER_UP	DAUER_STAT3_TARGETS_DN
GO_BILE_ACID_METABOLIC_PROCESS	GO_BILE_ACID_METABOLIC_PROCESS	CROONQUIST_STROMAL_STIMULATION_DN	DOANE_BREAST_CANCER_CLASSES_DN
GO_BRAIN_MORPHOGENESIS	GO_BROWN_FAT_CELL_DIFFERENTIATION	DAUER_STAT3_TARGETS_DN	DUTTA_APOPTOSIS_VIA_NFKB
GO_BROWN_FAT_CELL_DIFFERENTIATION	GO_CELL_MATURATION	DORN_ADENOVIRUS_INFECTION_32HR_UP	EINAV_INTERFERON_SIGNATURE_IN_CANCER
GO_CALCIIUM_INDEPENDENT_CELL_CELL_ADHESION_VIA_PLASMA_MEMBRANE_CELL_ADHESION_MOLECULES	GO_CELLULAR_IRON_ION_HOMEOSTASIS	DORN_ADENOVIRUS_INFECTION_48HR_UP	FARMER_BREAST_CANCER_CLUSTER_1
GO_CATECHOLAMINE_BINDING	GO_CHAPERONE_MEDIATED_PROTEIN_COMPLEX_ASSEMBLY	DUTTA_APOPTOSIS_VIA_NFKB	FERRANDO_LYL1_NEIGHBORS
GO_CELLULAR_IRON_ION_HOMEOSTASIS	GO_COMPLEMENT_ACTIVATION	EINAV_INTERFERON_SIGNATURE_IN_CANCER	GAUSSMANN_MLL_AF4_FUSION_TARGETS_F_DN
GO_CHAPERONE_MEDIATED_PROTEIN_COMPLEX_ASSEMBLY	GO_COMPLEMENT_ACTIVATION_ALTERNATIVE_PATHWAY	FIGUEROA_AML_METHYLATION_CLUSTER_5_DN	GO_ACETYLGALACTOSAMINYLT RANSFERASE_ACTIVITY
GO_CHYLOMICRON	GO_CYTOSOLIC_SMALL_RIBOSOMAL_SUBUNIT	FINETTI_BREAST_CANCER_KINOME_GREEN	GO_ACTIN_FILAMENT_POLYMERIZATION

Continued

Continued

Up-regulated in G3TM PKD		Down-regulated in G3TM PKD	
GO_COMPLEMENT_ACTIVATION	GO_DETECTION_OF_CHEMICAL_STIMULUS_INVOLVED_IN_SENSOR_PERCEPTION_OF_TASTE	FUNG_IL2_SIGNALING_2	GO_ACTIVATION_OF_CYSTEINE_TYPE_ENDOPEPTIDASE_ACTIVITY_INVOLVED_IN_APOPTOTIC_SIGNALING_PATHWAY
GO_COMPLEMENT_ACTIVATION_ALTERNATIVE_PATHWAY	GO_DYNEIN_BINDING	GAUSSMANN_MLL_AF4_FUSION_TARGETS_F_DN	GO_ADENYLATE_CYCLASE_ACTIVATING_DOPAMINE_RECEPTOR_SIGNALING_PATHWAY
GO_CYTOSOLIC_SMALL_RIBOSOMAL_SUBUNIT	GO_ERBB2_SIGNALING_PATHWAY	GAVIN_FOXP3_TARGETS_CLUSTER_T7	GO_ADENYLATE_CYCLASE_ACTIVATING_G_PROTEIN_COUPLED_RECEPTOR_SIGNALING_PATHWAY
GO_DETECTION_OF_CHEMICAL_STIMULUS_INVOLVED_IN_SENSOR_PERCEPTION_OF_TASTE	GO_FAT_SOLUBLE_VITAMIN_METABOLIC_PROCESS	GENTILE_UV_RESPONSE_CLUSTER_D1	GO_ADENYLATE_CYCLASE_MODULATING_G_PROTEIN_COUPLED_RECEPTOR_SIGNALING_PATHWAY
GO_DETOXIFICATION	GO_GAS_TRANSPORT	GO_14_3_3_PROTEIN_BINDING	GO_ADRENERGIC_RECEPTOR_SIGNALING_PATHWAY
GO_ENDOCYTTIC_VESICLE_LUMEN	GO_HUMORAL_IMMUNE_RESPONSE_MEDIATED_BY_CIRCULATING_IMMUNOGLOBULIN	GO_ACETYLGALACTOSAMINYLT RANSFERASE_ACTIVITY	GO_AXON_REGENERATION
GO_EPOXYGENASE_P450_PATHWAY	GO_HYDROLASE_ACTIVITY_ACTING_ON_CARBON_NITROGEN_BUT_NOT_PEPTIDE_BONDS_IN_LINEAR_AMIDINES	GO_ACROSOME_ASSEMBLY	GO_B_CELL_RECEPTOR_SIGNALING_PATHWAY
GO_FAT_SOLUBLE_VITAMIN_METABOLIC_PROCESS	GO_MAP_KINASE_KINASE_KINASE_ACTIVITY	GO_ACTIN_FILAMENT_POLYMERIZATION	GO_BASEMENT_MEMBRANE_ORGANIZATION
GO_HIGH_DENSITY_LIPOPROTEIN_PARTICLE	GO_MHC_CLASS_II_PROTEIN_COMPLEX_BINDING	GO_ACTIVATION_OF_ADENYLATE_CYCLASE_ACTIVITY	GO_BETA_1_3_GALACTOSYLTRANSFERASE_ACTIVITY
GO_HUMORAL_IMMUNE_RESPONSE_MEDIATED_BY_CIRCULATING_IMMUNOGLOBULIN	GO_MULTIVESICULAR_BODY_ORGANIZATION	GO_ACTIVATION_OF_CYSTEINE_TYPE_ENDOPEPTIDASE_ACTIVITY_INVOLVED_IN_APOPTOTIC_SIGNALING_PATHWAY	GO_CELLULAR_RESPONSE_TO_EXOGENOUS_DSRNA
GO_HYDROLASE_ACTIVITY_ACTING_ON_CARBON_NITROGEN_BUT_NOT_PEPTIDE_BONDS_IN_LINEAR_AMIDINES	GO_NEGATIVE_REGULATION_OF_ACUTE_INFLAMMATORY_RESPONSE	GO_ADENYLATE_CYCLASE_ACTIVATING_G_PROTEIN_COUPLED_RECEPTOR_SIGNALING_PATHWAY	GO_CELLULAR_RESPONSE_TO_PROSTAGLANDIN_E_STIMULUS
GO_INTRINSIC_COMPONENT_OF_MITOCHONDRIAL_OUTER_MEMBRANE	GO_NEGATIVE_REGULATION_OF_ANDROGEN_RECEPTOR_SIGNALING_PATHWAY	GO_ADENYLYLTRANSFERASE_ACTIVITY	GO_COPPER_ION_TRANSPORT
GO_MHC_CLASS_II_PROTEIN_COMPLEX_BINDING	GO_NEGATIVE_REGULATION_OF_CALCIIUM_ION_IMPORT	GO_ANTIGEN_BINDING	GO_CYTOLYSIS
GO_MITOCHONDRIAL_ATP_SYNTHESIS_COUPLED_PROTON_TRANSPORT	GO_NEGATIVE_REGULATION_OF_CARBOHYDRATE_METABOLIC_PROCESS	GO_B_CELL_ACTIVATION	GO_CYTOPLASMIC_SEQUESTERING_OF_TRANSCRIPTION_FACTOR
GO_MULTIVESICULAR_BODY_ORGANIZATION	GO_NEGATIVE_REGULATION_OF_HORMONE_SECRETION	GO_B_CELL_RECEPTOR_SIGNALING_PATHWAY	GO_DISRUPTION_OF_CELLS_OF_OTHER_ORGANISM
GO_NEGATIVE_REGULATION_OF_ACUTE_INFLAMMATORY_RESPONSE	GO_NEGATIVE_REGULATION_OF_PEPTIDE_SECRETION	GO_BETA_1_3_GALACTOSYLTRANSFERASE_ACTIVITY	GO_DISRUPTION_OF_CELLS_OF_OTHER_ORGANISM_INVOLVED_IN_SYMBIOTIC_INTERACTION
GO_NEGATIVE_REGULATION_OF_ANDROGEN_RECEPTOR_SIGNALING_PATHWAY	GO_NEGATIVE_REGULATION_OF_PROTEIN_OLIGOMERIZATION	GO_CELLULAR_COMPONENT_DISASSEMBLY_INVOLVED_IN_EXECUTION_PHASE_OF_APOPTOSIS	GO_DNA_TEMPLATED_TRANSCRIPTIONAL_PREINITIATION_COMPLEX_ASSEMBLY

Continued

Continued

Up-regulated in G3TM PKD		Down-regulated in G3TM PKD	
GO_NEGATIVE_REGULATION_OF_CALCIUM_ION_IMPORT	GO_NEGATIVE_REGULATION_OF_RELEASE_OF_CYTOCHROME_C_FROM_MITOCHONDRIA	GO_CELLULAR_RESPONSE_TO_ACID_CHEMICAL	GO_DOPAMINE_RECEPTOR_BINDING
GO_NEGATIVE_REGULATION_OF_HORMONE_SECRETION	GO_NUCLEOBASE_METABOLIC_PROCESS	GO_CELLULAR_RESPONSE_TO_EXOGENOUS_DSRNA	GO_DOPAMINE_RECEPTOR_SIGNALING_PATHWAY
GO_NEGATIVE_REGULATION_OF_LIPID_CATABOLIC_PROCESS	GO_NUCLEOSIDE_PHOSPHATE_CATABOLIC_PROCESS	GO_CELLULAR_RESPONSE_TO_GLUCOSE_STARVATION	GO_DRUG_BINDING
GO_NEGATIVE_REGULATION_OF_PEPTIDE_SECRETION	GO_ORGANIC_CYCLIC_COMPOUND_CATABOLIC_PROCESS	GO_CELLULAR_RESPONSE_TO_PROSTAGLANDIN_E_STIMULUS	GO_ENDOPLASMIC_RETICULUM_CHAPERONE_COMPLEX
GO_NEGATIVE_REGULATION_OF_RELEASE_OF_CYTOCHROME_C_FROM_MITOCHONDRIA	GO_OXYGEN_TRANSPORT	GO_CELLULAR_RESPONSE_TO_PROSTAGLANDIN_STIMULUS	GO_EPITHELIAL_STRUCTURE_MAINTENANCE
GO_NEGATIVE_REGULATION_OF_RESPONSE_TO_OXIDATIVE_STRESS	GO_PEPTIDE_ANTIGEN_BINDING	GO_COPPER_ION_TRANSPORT	GO_ERYTHROCYTE_DEVELOPMENT
GO_ORGAN_OR_TISSUE_SPECIFIC_IMMUNE_RESPONSE	GO_POSITIVE_REGULATION_OF_CARDIAC_MUSCLE_CONTRACTION	GO_CYCLIN_DEPENDENT_PROTEIN_SERINE_THREONINE_KINASE_INHIBITOR_ACTIVITY	GO_EXECUTION_PHASE_OF_APOPTOSIS
GO_OXIDOREDUCTASE_ACTIVITY_ACTING_ON_PAIRED_DONORS_WITH_INCORPORATION_OR_REDUCTION_OF_MOLECULAR_OXYGEN_REDUCED_FLAVIN_OR_FLAVOPROTEIN_AS_ONE_DONOR_AND_INCORPORATION_OF_ONE_ATOM_OF_OXYGEN	GO_POSITIVE_REGULATION_OF_CATECHOLAMINE_SECRETION	GO_CYTOPLASMIC_SEQUESTERING_OF_TRANSCRIPTION_FACTOR	GO GRANULOCYTE DIFFERENTIATION
GO_OXYGEN_BINDING	GO_POSITIVE_REGULATION_OF_TRANSCRIPTION_INITIATION_FROM_RNA_POLYMERASE_II_PROMOTER	GO_DEAMINASE_ACTIVITY	GO_INTERACTION_WITH_SYMBIONT
GO_OXYGEN_TRANSPORT	GO_PROTEIN_BINDING_INVOLVED_IN_PROTEIN_FOLDING	GO_DEFENSE_RESPONSE_TO_VIRUS	GO_ISOPRENOID_BINDING
GO_POSITIVE_REGULATION_OF_CARDIAC_MUSCLE_CONTRACTION	GO_REGULATION_OF_APPETITE	GO_DOPAMINE_RECEPTOR_BINDING	GO_LYMPHOID_PROGENITOR_CELL_DIFFERENTIATION
GO_POSITIVE_REGULATION_OF_FATTY_ACID_METABOLIC_PROCESS	GO_REGULATION_OF_CELL_PROJECTION_SIZE	GO_ENDOLYSOSOME	GO_MACROPHAGE_DIFFERENTIATION
GO_POSITIVE_REGULATION_OF_FATTY_ACID_OXIDATION	GO_REGULATION_OF_CELLULAR_AMINO_ACID_METABOLIC_PROCESS	GO_ENDOPLASMIC_RETICULUM_CHAPERONE_COMPLEX	GO_MAINTENANCE_OF_CELL_POLARITY
GO_POSITIVE_REGULATION_OF_LIPID_STORAGE	GO_REGULATION_OF_MICROTUBULE_BASED_MOVEMENT	GO_EPITHELIAL_STRUCTURE_MAINTENANCE	GO_MAINTENANCE_OF_GASTRO_INTESTINAL_EPITHELIUM
GO_POSITIVE_REGULATION_OF_RELEASE_OF_CYTOCHROME_C_FROM_MITOCHONDRIA	GO_REGULATION_OF_URINE_VOLUME	GO_EXTRINSIC_APOPTOTIC_SIGNALING_PATHWAY_VIA_DEATH_DOMAIN_RECEPTORS	GO_MAP_KINASE_ACTIVITY
GO_POSITIVE_REGULATION_OF_RESPONSE_TO_OXIDATIVE_STRESS	GO_RENAL_SYSTEM_PROCESS_INVOLVED_IN_REGULATION_OF_BLOOD_VOLUME	GO_FEMALE_GAMETE_GENERATION	GO_MULTICELLULAR_ORGANISMAL_MOVEMENT

Continued

Continued

Up-regulated in G3TM PKD		Down-regulated in G3TM PKD	
GO_POSITIVE_REGULATION_OF_TRANSCRIPTION_INITIATION_FROM_RNA_POLYMERASE_II_PROMOTER	GO_RESPONSE_TO_ACTIVITY	GO_G_PROTEIN_BETA_GAMMA_SUBUNIT_COMPLEX_BINDING	GO_NATURAL_KILLER_CELL_DIFFERENTIATION
GO_PROTEIN_BINDING_INVOLVED_IN_PROTEIN_FOLDING	GO_RESPONSE_TO_CAMP	GO_G_PROTEIN_COUPLED_RECE_PTOR_SIGNALING_PATHWAY_COUPLED_TO_CYCLIC_NUCLEOTIDE_SECOND_MESSENGER	GO_NECROTIC_CELL_DEATH
GO_PROTEIN_REFOLDING	GO_RESPONSE_TO_COLD	GO_GALACTOSYLTRANSFERASE_ACTIVITY	GO_NEGATIVE_REGULATION_OF_CALCIIUM_ION_TRANSMEMBRANE_TRANSPORT
GO_PROTON_TRANSPORTING_ATP_SYNTHASE_COMPLEX	GO_RESPONSE_TO_DIETARY_EXCESS	GO_GLYCOPROTEIN_CATABOLIC_PROCESS	GO_NEGATIVE_REGULATION_OF_GLYCOPROTEIN_BIOSYNTHETIC_PROCESS
GO_QUATERNARY_AMMONIUM_GROUP_BINDING	GO_RESPONSE_TO_MISFOLDED_PROTEIN	GO_GRANULOCYTE_DIFFERENTIATION	GO_NEGATIVE_REGULATION_OF_HOMEOSTATIC_PROCESS
GO_REACTIVE_OXYGEN_SPECIES_BIOSYNTHETIC_PROCESS	GO_RESPONSE_TO_SALT_STRESS	GO_GTPASE_ACTIVATING_PROTEIN_BINDING	GO_NEGATIVE_REGULATION_OF_INTERLEUKIN_1_PRODUCTION
GO_REACTIVE_OXYGEN_SPECIES_METABOLIC_PROCESS	GO_RETINA_HOMEOSTASIS	GO_I_KAPPAB_KINASE_NF_KAPPAB_SIGNALING	GO_NEGATIVE_REGULATION_OF_INTERLEUKIN_10_PRODUCTION
GO_REGULATION_OF_APPETITE	GO_RETINOL_DEHYDROGENASE_ACTIVITY	GO_ISOPRENOID_BINDING	GO_NEGATIVE_REGULATION_OF_INTRINSIC_APOPTOTIC_SIGNALING_PATHWAY
GO_REGULATION_OF_CELLULAR_AMINO_ACID_METABOLIC_PROCESS	GO_SENSORY_PERCEPTION_OF_TASTE	GO_JNK_CASCADE	GO_NEGATIVE_REGULATION_OF_INTRINSIC_APOPTOTIC_SIGNALING_PATHWAY_IN_RESPONSE_TO_DNA_DAMAGE
GO_REGULATION_OF_ENERGY_HOMEOSTASIS	GO_SEQUESTERING_OF_METAL_ION	GO_KINASE_INHIBITOR_ACTIVITY	GO_NEGATIVE_REGULATION_OF_LEUKOCYTE_APOPTOTIC_PROCESS
GO_REGULATION_OF_MICROTUBULE_BASED_MOVEMENT	GO_TETRAPYRROLE_BINDING	GO_KINASE_REGULATOR_ACTIVITY	GO_NEGATIVE_REGULATION_OF_LYASE_ACTIVITY
GO_REGULATION_OF_OXIDATIVE_STRESS_INDUCED_CELL_DEATH	GO_U1_SNRNP	GO_LYMPH_NODE_DEVELOPMENT	GO_NEGATIVE_REGULATION_OF_LYMPHOCYTE_APOPTOTIC_PROCESS
GO_REGULATION_OF_RELEASE_OF_CYTOCHROME_C_FROM_MITOCHONDRIA	GO_UBIQUITIN_LIKE_PROTEIN_CONJUGATING_ENZYME_BINDING	GO_LYMPHOCYTE_HOMEOSTASIS	GO_NEGATIVE_REGULATION_OF_MYELOID_CELL_APOPTOTIC_PROCESS
GO_REGULATION_OF_SEQUESTERING_OF_TRIGLYCERIDE	GO_VIRION_ASSEMBLY	GO_MAINTENANCE_OF_GASTROINTESTINAL_EPITHELIUM	GO_NEGATIVE_REGULATION_OF_OSTEOCLAST_DIFFERENTIATION
GO_REGULATION_OF_URINE_VOLUME	GOERING_BLOOD_HDL_CHOLESTEROL_QTL_CIS	GO_MEMBRANE_TUBULATION	GO_NEGATIVE_REGULATION_OF_RESPONSE_TO_BIOTIC_STIMULUS
GO_RENAL_SYSTEM_PROCESS_INVOLVED_IN_REGULATION_OF_BLOOD_VOLUME	HALLMARK_PANCREAS_BETA_CELLS	GO_MITOGEN_ACTIVATED_PROTEIN_KINASE_KINASE_BINDING	GO_NEGATIVE_REGULATION_OF_RESPONSE_TO_DNA_DAMAGE_STIMULUS
GO_RESPONSE_TO_CAMP	HALMOS_CEBPA_TARGETS_DN	GO_MITOTIC_SISTER_CHROMATID_COHESION	GO_NEGATIVE_REGULATION_OF_SIGNAL_TRANSDUCTION_BY_P53_CLASS_MEDIATOR

Continued

Continued

Up-regulated in G3TM PKD		Down-regulated in G3TM PKD	
GO_RESPONSE_TO_COLD	HOUSTIS_ROS	GO_MODULATION_BY_HOST_OF_VIRAL_PROCESS	GO_NEGATIVE_REGULATION_OF_STAT_CASCADE
GO_RESPONSE_TO_DIETARY_EXCESS	HUI_MAPK14_TARGETS_UP	GO_MRNA_TRANSCRIPTION	GO_NEGATIVE_REGULATION_OF_TRANSMEMBRANE_TRANSPORT
GO_RESPONSE_TO_MISFOLDED_PROTEIN	HWANG_PROSTATE_CANCER_MARKERS	GO_MRNA_TRANSCRIPTION_FROM_RNA_POLYMERASE_II_PROMOTER	GO_NEGATIVE_T_CELL_SELECTION
GO_RESPONSE_TO_OXYGEN_RADICAL	KANG_GLIS3_TARGETS	GO_NATURAL_KILLER_CELL_ACTIVATION	GO_NEURON_PROJECTION_REGENERATION
GO_RESPONSE_TO_PHENYLPROPANOID	KEGG_ADIPOCYTOKINE_SIGNALING_PATHWAY	GO_NATURAL_KILLER_CELL_DIFFERENTIATION	GO_NUCLEAR_INCLUSION_BODY
GO_RETINA_HOMEOSTASIS	KEGG_RETINOL_METABOLISM	GO_NECROTIC_CELL_DEATH	GO_NUCLEOTIDASE_ACTIVITY
GO_RETINOL_DEHYDROGENASE_ACTIVITY	KIM_BIPOLAR_DISORDER_OLIGODENDROCYTE_DENSITY_CORR_DN	GO_NEGATIVE_REGULATION_OF_HOMEOSTATIC_PROCESS	GO_PHOSPHOLIPASE_C_ACTIVATING_G_PROTEIN_COUPLED_RECEPTOR_SIGNALING_PATHWAY
GO_SENSORY_PERCEPTION_OF_TASTE	KIM_RESPONSE_TO_TSA_AND_DECITABINE_UP	GO_NEGATIVE_REGULATION_OF_LEUKOCYTE_APOPTOTIC_PROCESS	GO_PHOSPHOLIPASE_C_ACTIVITY
GO_SPERM_MOTILITY	LEE_LIVER_CANCER_ACOX1_UP	GO_NEGATIVE_REGULATION_OF_LIPID_BIOSYNTHETIC_PROCESS	GO_PHOSPHOTRANSFERASE_ACTIVITY_NITROGENOUS_GROUP_AS_ACCEPTOR
GO_TETRAPYRROLE_BINDING	MATZUK_SPERMATID_DIFFERENTIATION	GO_NEGATIVE_REGULATION_OF_LYMPHOCYTE_APOPTOTIC_PROCESS	GO_POLY_A_MRNA_EXPORT_FROM_NUCLEUS
GO_U1_SNRNP	MEISSNER_ES_ICP_WITH_H3K4ME3_AND_H3K27ME3	GO_NEGATIVE_REGULATION_OF_LYMPHOCYTE_MEDIATED_IMMUNITY	GO_POSITIVE_REGULATION_OF_B_CELL_PROLIFERATION
GO_UBIQUITIN_LIKE_PROTEIN_CONJUGATING_ENZYME_BINDING	MIKKELSEN_IPS_LCP_WITH_H3K27ME3	GO_NEGATIVE_REGULATION_OF_MYELOID_CELL_APOPTOTIC_PROCESS	GO_POSITIVE_REGULATION_OF_CAMP_MEDIATED_SIGNALING
GO_VIRION_ASSEMBLY	MIKKELSEN_MEF_HCP_WITH_H3_UNMETHYLATED	GO_NEGATIVE_REGULATION_OF_OSTEOCLAST_DIFFERENTIATION	GO_POSITIVE_REGULATION_OF_ERYTHROCYTE_DIFFERENTIATION
HALMOS_CEBPA_TARGETS_DN	NGUYEN_NOTCH1_TARGETS_UP	GO_NEGATIVE_REGULATION_OF_RESPONSE_TO_BIOTIC_STIMULUS	GO_POSITIVE_REGULATION_OF_INTRINSIC_APOPTOTIC_SIGNALING_PATHWAY
HEDVAT_ELF4_TARGETS_UP	NIKOLSKY_BREAST_CANCER_8Q23_Q24_AMPLICON	GO_NEGATIVE_REGULATION_OF_RESPONSE_TO_DNA_DAMAGE_STIMULUS	GO_POSITIVE_REGULATION_OF_LYASE_ACTIVITY
HOUSTIS_ROS	PEDERSEN_METASTASIS_BY_ERBB2_ISOFORM_6	GO_NEGATIVE_REGULATION_OF_STAT_CASCADE	GO_POSITIVE_REGULATION_OF_LYMPHOCYTE_MIGRATION
HOWLIN_CITED1_TARGETS_2_UP	REACTOME_APOPTOTIC_CLEAVAGE_OF_CELL_ADHESION_PROTEINS	GO_NEGATIVE_REGULATION_OF_TRANSMEMBRANE_TRANSPORT	GO_POSITIVE_REGULATION_OF_MEMBRANE_INVAGINATION
HUI_MAPK14_TARGETS_UP	REACTOME_COMPLEMENT_CASCADE	GO_NEGATIVE_REGULATION_OF_TYPE_I_INTERFERON_PRODUCTION	GO_POSITIVE_REGULATION_OF_NUCLEOTIDE_METABOLIC_PROCESS

Continued

Continued

Up-regulated in G3TM PKD		Down-regulated in G3TM PKD	
HWANG_PROSTATE_CANCER_MARKERS	REACTOME_INITIAL_TRIGGERING_OF_COMPLEMENT	GO_NUCLEOTIDASE_ACTIVITY	GO_POSITIVE_REGULATION_OF_OXIDATIVE_STRESS_INDUCED_CELL_DEATH
KANG_GLI33_TARGETS	REACTOME_REGULATION_OF_RHEB_GTPASE_ACTIVITY_BY_AMPK	GO_OLIGOSACCHARIDE_BIOSYNTHETIC_PROCESS	GO_POSITIVE_REGULATION_OF_PROTEIN_DEACETYLATION
KEGG_PARKINSONS_DISEASE	REACTOME_TANDEM_PORE_DOMAIN_POTASSIUM_CHANNELS	GO_OOCYTE_MATURATION	GO_POSITIVE_REGULATION_OF_THYMOCYTE_AGGREGATION
KEGG_TASTE_TRANSDUCTION	SHANK_TAL1_TARGETS_DN	GO_PARTURITION	GO_PROSTANOID_METABOLIC_PROCESS
KIM_BIPOLAR_DISORDER_OLIGODENDROCYTE_DENSITY_CORR_DN	SUBTIL_PROGESTIN_TARGETS	GO_PHOSPHATE_ION_BINDING	GO_PROTEIN_DESTABILIZATION
KIM_RESPONSE_TO_TSA_AND_DECITABINE_UP	VALK_AML_CLUSTER_10	GO_PHOSPHATIDIC_ACID_BINDING	GO_PROTEIN_HOMOTRIMERIZATION
LEE_LIVER_CANCER_ACOX1_UP	VALK_AML_CLUSTER_15	GO_PHOSPHATIDYLINOSITOL_4_PHOSPHATE_BINDING	GO_PYRIMIDINE_CONTAINING_COMPOUND_SALVAGE
MATZUK_SPERMATID_DIFFERENTIATION	VALK_AML_WITH_EVI1	GO_PHOSPHOLIPASE_C_ACTIVATING_G_PROTEIN_COUPLED_RECEPTOR_SIGNALING_PATHWAY	GO_REGULATION_OF_ADENYLATE_CYCLASE_ACTIVITY
MEISSNER_ES_ICP_WITH_H3K4ME3_AND_H3K27ME3	WANG_BARRETTS_ESOPHAGUS_AND_ESOPHAGUS_CANCER_UP	GO_PHOSPHOLIPASE_C_ACTIVITY	GO_REGULATION_OF_ALPHA_AMINO_3_HYDROXY_5_METHYL_4_ISOXAZOLE_PROPIONATE_SELECTIVE_Glutamate_RECEPTOR_ACTIVITY
MIKKELSEN_MEF_HCP_WITH_H3_UNMETHYLATED	WANG_PROSTATE_CANCER_ANDROGEN_INDEPENDENT	GO_PHOSPHOTRANSFERASE_ACTIVITY_NITROGENOUS_GROUP_AS_ACCEPTOR	GO_REGULATION_OF_B_CELL_RECEPTOR_SIGNALING_PATHWAY
NGUYEN_NOTCH1_TARGETS_UP	WANG_RESPONSE_TO_ANDROGEN_UP	GO_POSITIVE_REGULATION_OF_ALCOHOL_BIOSYNTHETIC_PROCESS	GO_REGULATION_OF_BONE_DEVELOPMENT
NIKOLSKY_BREAST_CANCER_8Q23_Q24_AMPLICON	WEBER_METHYLATED_HCP_IN_SPERM_DN	GO_POSITIVE_REGULATION_OF_B_CELL_DIFFERENTIATION	GO_REGULATION_OF_BONE_RESORPTION
PEDERSEN_METASTASIS_BY_ERBB2_ISOFORM_6	YAO_TEMPORAL_RESPONSE_TO_PROGESTERONE_CLUSTER_10	GO_POSITIVE_REGULATION_OF_B_CELL_PROLIFERATION	GO_REGULATION_OF_DEFENSE_RESPONSE_TO_VIRUS_BY_HOST
REACTOME_COMPLEMENT_CASCADE	YAO_TEMPORAL_RESPONSE_TO_PROGESTERONE_CLUSTER_5	GO_POSITIVE_REGULATION_OF_CELLULAR_EXTRAVASATION	GO_REGULATION_OF_ERYTHROCYTE_DIFFERENTIATION
REACTOME_FORMATION_OF_ATP_BY_CHEMIOSMOTIC_COUPLING	YAO_TEMPORAL_RESPONSE_TO_PROGESTERONE_CLUSTER_9	GO_POSITIVE_REGULATION_OF_ERYTHROCYTE_DIFFERENTIATION	GO_REGULATION_OF_FEVER_GENERATION
REACTOME_INITIAL_TRIGGERING_OF_COMPLEMENT	ZHOU_PANCREATIC_EXOCRINE_PROGENITOR	GO_POSITIVE_REGULATION_OF_INTERFERON_ALPHA_PRODUCTI ON	GO_REGULATION_OF_INTRINSIC_APOPTOTIC_SIGNALING_PATHWAY
REACTOME_OXYGEN_DEPENDENT_PROLINE_HYDROXYLATION_OF_HYPOXIA_INDUCIBLE_FACTOR_ALPHA		GO_POSITIVE_REGULATION_OF_INTERFERON_BETA_PRODUCTION	GO_REGULATION_OF_INTRINSIC_APOPTOTIC_SIGNALING_PATHWAY_BY_P53_CLASS_MEDIATOR
REACTOME_REGULATION_OF_RHEB_GTPASE_ACTIVITY_BY_AMPK		GO_POSITIVE_REGULATION_OF_LAMELLIPODIUM_ASSEMBLY	GO_REGULATION_OF_INTRINSIC_APOPTOTIC_SIGNALING_PATHWAY_IN_RESPONSE_TO_DNA_DAMAGE

Continued

Continued

Up-regulated in G3TM PKD	Down-regulated in G3TM PKD	
REACTOME_RESPIRATORY_ELECTRON_TRANSPORT	GO_POSITIVE_REGULATION_OF_LYASE_ACTIVITY	GO_REGULATION_OF_INTRINSIC_APOPTOTIC_SIGNALING_PATHWAY_IN_RESPONSE_TO_DNA_DAMAGE_BY_P53_CLASS_MEDIATOR
REACTOME_RESPIRATORY_ELECTRON_TRANSPORT_ATP_SYNTHESIS_BY_CHEMIOSMOTIC_COUPLING_AND_HEAT_PRODUCTION_BY_UNCOUPLING_PROTEINS	GO_POSITIVE_REGULATION_OF_LYMPHOCYTE_MIGRATION	GO_REGULATION_OF_LYASE_ACTIVITY
REACTOME_TANDEM_PORE_DOMAIN_POTASSIUM_CHANNELS	GO_POSITIVE_REGULATION_OF_MEMBRANE_INVAGINATION	GO_REGULATION_OF_MEMBRANE_INVAGINATION
REACTOME_TIGHT_JUNCTION_INTERACTIONS	GO_POSITIVE_REGULATION_OF_NATURAL_KILLER_CELL_MEDIATED_IMMUNITY	GO_REGULATION_OF_PROTEIN_TYROSINE_KINASE_ACTIVITY
REACTOME_XENOBIOTICS	GO_POSITIVE_REGULATION_OF_NUCLEOTIDE_METABOLIC_PROCESS	GO_REGULATION_OF_RECEPTOR_BINDING
SHANK_TAL1_TARGETS_DN	GO_POSITIVE_REGULATION_OF_PROTEIN_AUTOPHOSPHORYLATION	GO_REGULATION_OF_T_CELL_APOPTOTIC_PROCESS
SUBTIL_PROGESTIN_TARGETS	GO_POSITIVE_REGULATION_OF_RESPONSE_TO_CYTOKINE_STIMULUS	GO_REGULATION_OF_THYMOCYTE_AGGREGATION
VALK_AML_CLUSTER_10	GO_POSITIVE_REGULATION_OF_T_CELL_MEDIATED_IMMUNITY	GO_REGULATION_OF_THYMOCYTE_APOPTOTIC_PROCESS
VALK_AML_WITH_EV1	GO_POSITIVE_REGULATION_OF_THYMOCYTE_AGGREGATION	GO_RESPONSE_TO_SALT
VANLOO_SP3_TARGETS_DN	GO_PROSTANOID_BIOSYNTHETIC_PROCESS	GO_RETINAL_BINDING
WAMUNYOKOLI_OVARIAN_CANCER_LMP_UP	GO_PROSTANOID_METABOLIC_PROCESS	GO_SKELETAL_MUSCLE_CONTRACTION
WANG_BARRETTS_ESOPHAGUS_AND_ESOPHAGUS_CANCER_UP	GO_PROTEIN_C_TERMINUS_BINDING	GO_SULFATION
WEBER_METHYLATED_HCP_IN_SPERM_DN	GO_PROTEIN_DESTABILIZATION	GO_SUMO_TRANSFERASE_ACTIVITY
YAO_TEMPORAL_RESPONSE_TO_PROGESTERONE_CLUSTER_10	GO_PYRIMIDINE_CONTAINING_COMPOUND_SALVAGE	GO_SUPEROXIDE_METABOLIC_PROCESS
YAO_TEMPORAL_RESPONSE_TO_PROGESTERONE_CLUSTER_5	GO_REGULATION_OF_ACTIVATED_T_CELL_PROLIFERATION	GO_THYMIC_T_CELL_SELECTION
YAO_TEMPORAL_RESPONSE_TO_PROGESTERONE_CLUSTER_9	GO_REGULATION_OF_ANTIGEN_PROCESSING_AND_PRESENTATION	GO_THYMOCYTE_AGGREGATION
	GO_REGULATION_OF_B_CELL_PROLIFERATION	GO_TRANSCRIPTIONAL_REPRESSOR_ACTIVITY_RNA_POLYMERASE_II_CORE_PROMOTER_PROXIMAL_REGION_SEQUENCE_SPECIFIC_BINDING
	GO_REGULATION_OF_B_CELL_RECEPTOR_SIGNALING_PATHWAY	GO_XENOPHAGY

Continued

Continued

Up-regulated in G3TM PKD	Down-regulated in G3TM PKD	
	GO_REGULATION_OF_BONE_DEVELOPMENT	HANSON_HRAS_SIGNALING_VIA_NFKB
	GO_REGULATION_OF_BONE_REMODELING	HERNANDEZ_MITOTIC_ARREST_BY_DOCETAXEL_2_UP
	GO_REGULATION_OF_BONE_RESORPTION	HOFMANN_MYELODYSPLASTIC_SYNDROM_HIGH_RISK_DN
	GO_REGULATION_OF_ERYTHROCYTE_DIFFERENTIATION	HOFMANN_MYELODYSPLASTIC_SYNDROM_RISK_DN
	GO_REGULATION_OF_FEVER_GENERATION	HOLLEMAN_DAUNORUBICIN_B_ALL_DN
	GO_REGULATION_OF_INTERFERON_ALPHA_PRODUCTION	HOLLEMAN_VINCRISTINE_RESISTANCE_ALL_DN
	GO_REGULATION_OF_INTERFERON_BETA_PRODUCTION	HUMMERICH_BENIGN_SKIN_TUMOR_DN
	GO_REGULATION_OF_LYASE_ACTIVITY	HUMMERICH_MALIGNANT_SKIN_TUMOR_DN
	GO_REGULATION_OF_LYMPHOCYTE_CHEMOTAXIS	IYENGAR_RESPONSE_TO_ADIPOCYTE_FACTORS
	GO_REGULATION_OF_MEMBRANE_INVAGINATION	KAYO_CALORIE_RESTRICTION_MUSCLE_UP
	GO_REGULATION_OF_MRNA_CATABOLIC_PROCESS	KEGG_AMYOTROPHIC_LATERAL_SCLEROSIS_ALS
	GO_REGULATION_OF_NITRIC_OXIDE_SYNTHASE_BIOSYNTHETIC_PROCESS	KORKOLA_CHORIOCARCINOMA_DN
	GO_REGULATION_OF_PROTEIN_TYROSINE_KINASE_ACTIVITY	KRIEG_KDM3A_TARGETS_NOT_HYPOXIA
	GO_REGULATION_OF_T_CELL_APOPTOTIC_PROCESS	KUROKAWA_LIVER_CANCER_CHEMOTHERAPY_UP
	GO_REGULATION_OF_T_CELL_CHEMOTAXIS	LU_TUMOR_ENDOTHELIAL_MARKERS_UP
	GO_REGULATION_OF_T_CELL_MEDIATED_IMMUNITY	LU_TUMOR_VASCULATURE_UP
	GO_REGULATION_OF_T_CELL_MIGRATION	MA_MYELOID_DIFFERENTIATION_UP
	GO_REGULATION_OF_TOLL_LIKE_RECEPTOR_SIGNALING_PATHWAY	MATZUK_MALE_REPRODUCTION_SERTOLI
	GO_REGULATION_OF_TRANSCRIPTION_INITIATION_FROM_RNA_POLYMERASE_II_PROMOTER	MATZUK_OVULATION
	GO_REGULATION_OF_TYPE_I_INTERFERON_MEDIATED_SIGNALING_PATHWAY	MEISSNER_NPC_ICP_WITH_H3K4ME3
	GO_REGULATION_OF_TYPE_I_INTERFERON_PRODUCTION	MMS_MOUSE_LYMPH_HIGH_4HRS_UP
	GO_RESPONSE_TO_ACIDIC_PH	MOSERLE_IFNA_RESPONSE

Continued

Continued

Up-regulated in G3TM PKD	Down-regulated in G3TM PKD	
	GO_RESPONSE_TO_EXOGENOUS_DSRNA	NAKAMURA_LUNG_CANCER_DIFFERENTIATION_MARKERS
	GO_RESPONSE_TO_MURAMYL_DIPEPTIDE	NIKOLSKY_BREAST_CANCER_1Q21_AMPLICON
	GO_RESPONSE_TO_PLATELET_DERIVED_GROWTH_FACTOR	PID_LPA4_PATHWAY
	GO_RESPONSE_TO_VIRUS	PID_PI3KCI_PATHWAY
	GO_RETINAL_BINDING	RADAEVA_RESPONSE_TO_IFNA1_UP
	GO_RETINOL_BINDING	REACTOME_ADENYLATE_CYCLASE_ACTIVATING_PATHWAY
	GO_RNA_DESTABILIZATION	REACTOME_ADENYLATE_CYCLASE_INHIBITORY_PATHWAY
	GO_SUMO_TRANSFERASE_ACTIVITY	REACTOME_DSCAM_INTERACTIONS
	GO_THYMOCYTE_AGGREGATION	REACTOME_G_ALPHA_Z_SIGNALLING_EVENTS
	GO_THYROID_HORMONE_RECEPTOR_BINDING	REACTOME_INTRINSIC_PATHWAY_FOR_APOPTOSIS
	GO_TOLL_LIKE_RECEPTOR_4_SIGNALING_PATHWAY	REACTOME_PLATELET_ADHESION_TO_EXPOSED_COLLAGEN
	GO_TRANSCRIPTION_FACTOR_ACTIVITY_RNA_POLYMERASE_II_CORE_PROMOTER_SEQUENCE_SPECIFIC	REACTOME_PROSTACYCLIN_SIGNALLING_THROUGH_PROSTACYCLIN_RECEPTOR
	GO_TUMOR_NECROSIS_FACTOR_RECEPTOR_BINDING	REACTOME_REGULATION_OF_KIT_SIGNALING
	GO_TUMOR_NECROSIS_FACTOR_RECEPTOR_SUPERFAMILY_BINDING	REACTOME_RIP_MEDIATED_NFKB_ACTIVATION_VIA_DAI
	GRANDVAUX_IFN_RESPONSE_NOT_VIA_IRF3	REACTOME_TAK1_ACTIVATES_NFKB_BY_PHOSPHORYLATION_AND_ACTIVATION_OF_IKKS_COMPLEX
	HALLMARK_INTERFERON_ALPHA_RESPONSE	REACTOME_TRAF6_MEDIATED_NFKB_ACTIVATION
	HALLMARK_INTERFERON_GAMMA_RESPONSE	RICKMAN_HEAD_AND_NECK_CANCER_C
	HANSON_HRAS_SIGNALING_VIA_NFKB	RODRIGUES_THYROID_CARCINOMA_UP
	HOFMANN_MYELODYSPLASTIC_SYNDROM_HIGH_RISK_DN	SCHEIDEREIT_IKK_TARGETS
	HOFMANN_MYELODYSPLASTIC_SYNDROM_RISK_DN	SCHLESINGER_METHYLATED_IN_COLON_CANCER
	HOLLEMAN_ASPARAGINASE_RESISTANCE_B_ALL_DN	SHIN_B_CELL_LYMPHOMA_CLUSTER_2
	IYENGAR_RESPONSE_TO_ADIPOCYTE_FACTORS	SIG_CD40PATHWAYMAP

Continued

Continued

Up-regulated in G3TM PKD	Down-regulated in G3TM PKD
KEGG_GLYCOSAMINOGLYCAN_BIOSYNTHESIS_CHONDROITIN_SULFATE	SPIELMAN_LYMPHOBLAST_EUROPEAN_VS_ASIAN_2FC_DN
KORKOLA_CHORIOCARCINOMA_DN	ST_B_CELL_ANTIGEN_RECEPTOR
KRIEG_KDM3A_TARGETS_NOT_HYPOXIA	ST_T_CELL_SIGNAL_TRANSDUCTION
KUROKAWA_LIVER_CANCER_CHEMOTHERAPY_UP	XU_CREBBP_TARGETS_DN
KYNG_WERNER_SYNDROM_UP	ZEMBUTSU_SENSITIVITY_TO_MITOMYCIN
LEE_CALORIE_RESTRICTION_MUSCLE_DN	ZHAN_LATE_DIFFERENTIATION_GENES_DN
LU_TUMOR_ENDOTHELIAL_MARKERS_UP	ZHOU_INFLAMMATORY_RESPONSE_FIMA_DN
LU_TUMOR_VASCULATURE_UP	
MA_MYELOID_DIFFERENTIATION_UP	
MAHADEVAN_RESPONSE_TO_MP470_UP	
MARIADASON_RESPONSE_TO_CURCUMIN_SULINDAC_7	
MATZUK_MALE_REPRODUCTION_SERTOLI	
MATZUK_OVULATION	
MOSERLE_IFNA_RESPONSE	
MULLIGHAN_MLL_SIGNATURE_2_UP	
NAKAMURA_ADIPOGENESIS_EARLY_UP	
OUELLET_OVARIAN_CANCER_INVASIVE_VS_LMP_DN	
PARK_TRETINOIN_RESPONSE	
PID_EPO_PATHWAY	
PID_LPA4_PATHWAY	
PID_PI3KCI_PATHWAY	
PID_S1P_S1P3_PATHWAY	
PID_WNT_NONCANONICAL_PATHWAY	
RADAEVA_RESPONSE_TO_IFNA1_UP	
RASHI_RESPONSE_TO_IONIZING_RADIATION_4	
RAY_TUMORIGENESIS_BY_ERBB2_CDC25A_UP	

Continued

Continued

Up-regulated in G3TM PKD	Down-regulated in G3TM PKD
	REACTOME_ACTIVATION_OF_IRF3_IRF7_MEDIATED_BY_TBK1_IKK_EPSILON
	REACTOME_ADENYLATE_CYCLASE_ACTIVATING_PATHWAY
	REACTOME_ADENYLATE_CYCLASE_INHIBITORY_PATHWAY
	REACTOME_APOPTOSIS
	REACTOME_APOPTOTIC_EXECUTION_PHASE
	REACTOME_DSCAM_INTERACTIONS
	REACTOME_EARLY_PHASE_OF_HIV_LIFE_CYCLE
	REACTOME_IL_2_SIGNALING
	REACTOME_IL_3_5_AND_GM-CSF_SIGNALING
	REACTOME_IL_RECEPTOR_SHC_SIGNALING
	REACTOME_PD1_SIGNALING
	REACTOME_PHOSPHORYLATION_OF_CD3_AND_TCR_ZETA_CHAINS
	REACTOME_REGULATION_OF_KIT_SIGNALING
	REACTOME_RIP_MEDIATED_NFKB_ACTIVATION_VIA_DAI
	REACTOME_TAK1_ACTIVATES_NFKB_BY_PHOSPHORYLATION_AND_ACTIVATION_OF_IKKS_COMPLEX
	REACTOME_TRAF6_MEDIATED_INDUCTION_OF_TAK1_COMPLEX
	REACTOME_TRAF6_MEDIATED_NFKB_ACTIVATION
	REACTOME_TRAFFICKING_AND_PROCESSING_OF_ENDOSOMAL_TLR
	RODRIGUES_THYROID_CARCINOMA_UP
	ROSS_AML_WITH_CFBF_MYH11_FUSION
	SANA_RESPONSE_TO_IFNG_UP
	SCHEIDEREIT_IKK_TARGETS
	SIG_PIP3_SIGNALING_IN_CARDIAC_MYOCYTES

Continued

Continued

Up-regulated in G3TM PKD	Down-regulated in G3TM PKD
	ST_B_CELL_ANTIGEN_RECEPTOR
	ST_T_CELL_SIGNAL_ TRANSDUCTION
	ST_TUMOR_NECROSIS_FACTOR_ PATHWAY
	TONKS_TARGETS_OF_RUNX1_ RUNX1T1_FUSION_ ERYTHROCYTE_DN
	TURASHVILI_BREAST_NORMAL_ DUCTAL_VS_LOBULAR_UP
	WU_HBX_TARGETS_3_UP
	WUNDER_INFLAMMATORY_RES PONSE_AND_CHOLESTEROL_UP
	XU_AKT1_TARGETS_6HR
	XU_CREBBP_TARGETS_DN
	YANG_BCL3_TARGETS_UP
	ZEMBUTSU_SENSITIVITY_TO_ NIMUSTINE
	ZHAN_LATE_DIFFERENTIATION_ GENES_DN
	ZHAN_MULTIPLE_MYELOMA_ HP_UP
	ZHONG_SECRETOME_OF_LUNG_ CANCER_AND_MACROPHAGE
	ZHOU_INFLAMMATORY_ RESPONSE_FIMA_DN

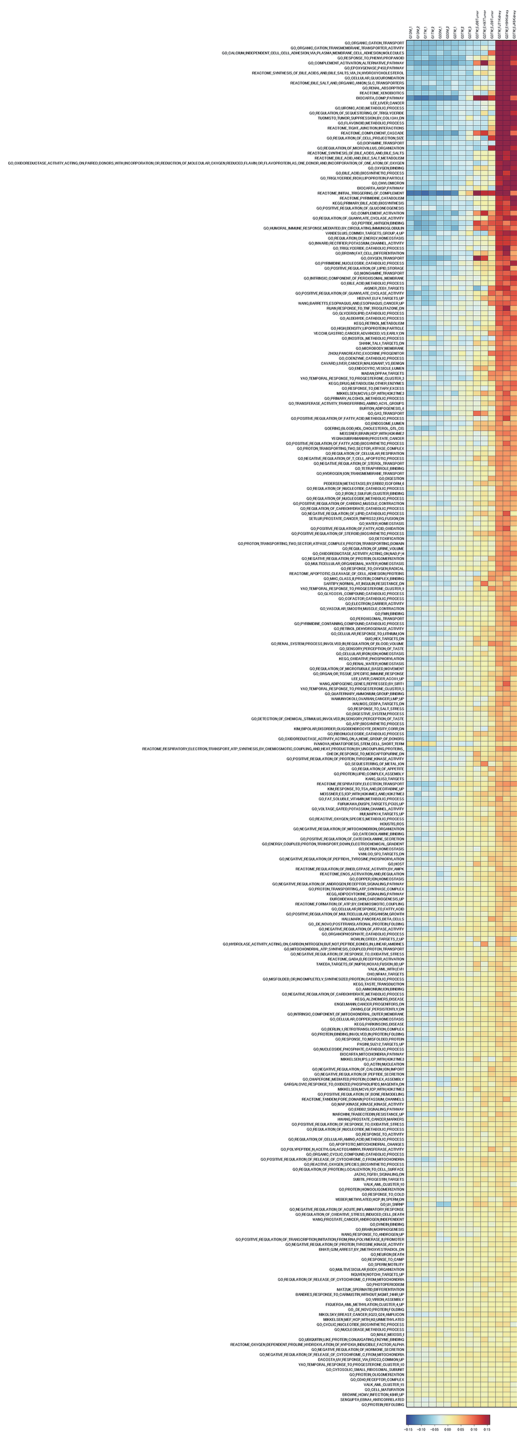


Figure S1 A heatmap of gene expression profiles (ssGSEA analysis results of the RNA-seq data using Hallmark, C2, and C5 datasets) in MEFs from G1DM, G2DM, G3DM, G1TM, G2TM, and G3TM mice, as well as the tumors and cystic kidneys from G3TM mice. The pathways were ranked by scores, showing upregulation in cystic kidney, as well as in the tumor and G3TM MEFs.

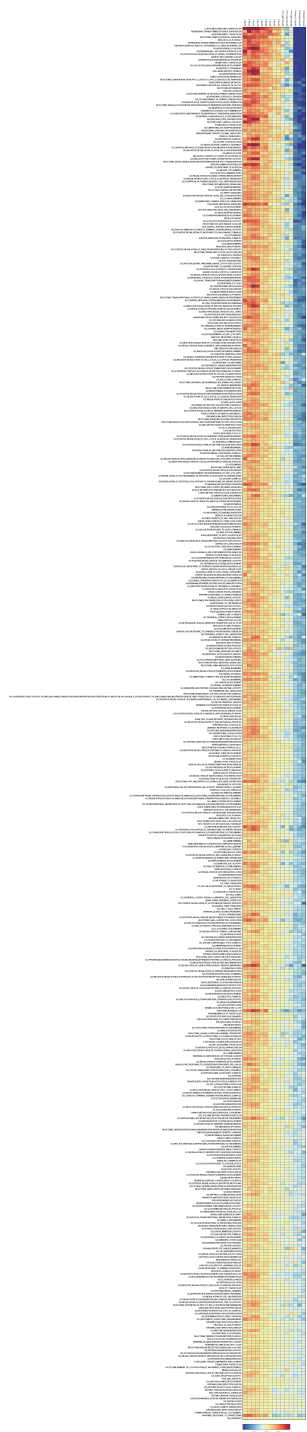


Figure S2 A heatmap of gene expression profiles (ssGSEA analysis results of the RNA-seq data using Hallmark, C2, and C5 datasets) in MEFs from G1DM, G2DM, G3DM, G1TM, G2TM, and G3TM mice, as well as tumors and cystic kidneys from G3TM mice. The pathways were ranked by scores showing the downregulation in the cystic kidney, as well as in tumor and in G3TM MEFs.